Resonance Raman and Time-Resolved Resonance Raman Evidence for Enhanced Localization in the ^{3}MLCT States of Ruthenium(II) Complexes with the Inherently Asymmetric Ligand 2-(2-Pyridyl)pyrazine

Gerald D. Danzer, Janus A. Golus, and James R. Kincaid*

Contribution from the Chemistry Department, Marquette University, Milwaukee, Wisconsin 53233

Received January 27, 1993®

Abstract: The resonance Raman (RR) and time-resolved resonance Raman (TR^3) spectra of ruthenium(II) complexes containing the inherently asymmetric 2-(2-pyridyl)pyrazine (pypz) and its selectively deuteriated analogue are reported. The spectrum of the ground-state species is interpretable in terms of vibrationally isolated fragments with the exception of several modes which involve the interring and adjacent bonds. More importantly, the TR^3 spectra of the (triplet) metal-to-ligand-charge-transfer state are shown to be consistent with the presence of a coordinated pypz in which the electronic charge is polarized toward the pyrazine fragment. A detailed discussion of the spectral analysis which leads to this conclusion is provided, and the potential implication of the effect for the design of practical devices is discussed.

Introduction

The potential utility of divalent ruthenium complexes of polypyridines and related ligands as components of practical solar energy conversion devices has generated intense interest and activity in the study of their relatively long-lived (triplet) metal-to-ligand-charge-transfer (^{3}MLCT) excited states.[1] In order to design and efficiently exploit this class of molecules for practical systems, a detailed understanding of the nature and reactivity of these excited states is required. An issue of fundamental importance, of course, is the electronic distribution of the ^{3}MLCT state.

A major breakthrough was made by Dallinger, Woodruff, and co-workers, who demonstrated the powerful utility of time-resolved resonance Raman (TR^3) methods for the direct interrogation of excited-state structures and dynamics of these systems.[2] That work, which was soon corroborated by similar studies of related systems,[3] confirmed earlier proposals[1c,4] which suggested that the excited-state electron density was essentially localized on a single chelate ring in the tris(bipyridine)(bpy) complex, i.e., the proper formulation of the excited state is $[Ru^{3+}(bpy)_2(bpy^-)]^{2+}$. Following this early lead, our group,[5] as well as Mabrouk and Wrighton,[6] used TR^3 methods to demonstrate that in tris-ligated, bis-heteroleptic complexes (such as $Ru(bpy)_2(dmb)^{2+}$), the ^{3}MLCT electron density may be selectively localized on a particular chelate ligand. More recently, we have shown that in heteroleptic complexes comprised of bipyridine and bipyrazine (bpz) ligands, there is specific population of the bipyrazine-centered ^{3}MLCT state, even in the case of $Ru(bpy)_2(bpz)^{2+}$.[7] Thus, TR^3 methods provide an especially effective and relatively convenient probe of the nature of symmetric and asymmetric complexes of this class.

Thus far, relatively little attention has been directed toward complexes comprised of inherently asymmetric polypyridine ligands, i.e., ligands which are themselves asymmetric, such as monosubstituted bipyridines.[8] In these cases, of course, there exists the possibility that the "localized" ^{3}MLCT state can experience further localization on a particular fragment of the chelate ligand. While no detailed studies of the excited states of such systems have yet been reported, studies of the electrochemically reduced complexes (which serve as models of the excited state) imply that such localization effects are indeed possible.[8b]

In the present work, we have conducted detailed resonance Raman (RR) and TR^3 studies of the ruthenium complexes of the inherently asymmetric ligand, 2-(2-pyridyl)pyrazine (pypz). The results provide definitive evidence that the ^{3}MLCT-state electron density is highly polarized toward the pyrazine fragment of the chelate.

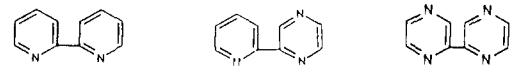

bpy pypz bpz

Experimental Section

Preparation of Compounds. A. Ligands. The ligand 2-(2-pyridyl)-pyrazine was prepared by the reductive coupling of equal molar amounts of freshly distilled 2-chloropyridine (Aldrich) and 2-chloropyrazine (Aldrich) using a previously reported procedure for pyridine coupling.[9] The ligand was purified to remove the 2,2′-bipyridine and 2,2′-bipyrazine byproducts by column chromatography on silica gel using hexane–diethyl ether (1:1) as the eluent. The ligand 3,5-dideuterio-2-(2-pyridyl)pyrazine was prepared by the reductive coupling of 3,5-dideuterio-2-chloropyridine and 2-chloropyrazine in a similar manner as for pypz, where 3,5-dideuterio-2-chloropyridine was prepared as described previously.[9a]

The predeuteriated 2,2′-bipyridine ligand (bpy-d_8) was prepared using a previously reported procedure,[10] and the 2,2′-bipyridine ligand was purchased from Aldrich Chemical Co.

® Abstract published in *Advance ACS Abstracts,* September 1, 1993.

(1) (a) Juris, A.; Balzani, V.; Barigelletti, F.; Campagna, S.; Belser, P.; Von Zelewesky, A. *Coord. Chem. Rev.* **1988**, *84*, 85. (b) Kalyanasundaram, K. *Coord. Chem. Rev.* **1982**, *46*, 159. (c) DeArmond, M. K.; Carlin, C. M. *Coord. Chem. Rev.* **1981**, *36*, 325. (d) Kalyanasundaram, K.; Grätzel, M.; Pelizetti, E. *Coord. Chem. Rev.* **1986**, *69*, 57. (e) Meyer, T. J. *Pure Appl. Chem.* **1986**, *58*, 1193.

(2) Bradley, P. G.; Kress, N.; Hornberger, B. A.; Dallinger, R. F.; Woodruff, W. H. *J. Am. Chem. Soc.* **1981**, *103*, 7441.

(3) (a) Smothers, W. K.; Wrighton, M. S. *J. Am. Chem. Soc.* **1983**, *105*, 1067. (b) McClanahan, S.; Hayes, T.; Kincaid, J. *J. Am. Chem. Soc.* **1983**, *103*, 4486.

(4) Sutin, N.; Creutz, C. *Adv. Chem. Ser.* **1978**, *138*, 1.

(5) McClanahan, S. F.; Dallinger, R. F.; Holler, F. J.; Kincaid, J. R. *J. Am. Chem. Soc.* **1985**, *107*, 4853.

(6) Marbrouk, P. A.; Wrighton, M. S. *Inorg. Chem.* **1986**, *25*, 526.

(7) Danzer, G. D.; Kincaid, J. R. *J. Phys. Chem.* **1990**, *94*, 3976.

(8) (a) Rilema, D. P.; Blanton, C. B.; Shaver, R. J.; Jackman, D. C.; Boldaji, M.; Bundy, S.; Worl, L. A.; Meyer, T. J. *Inorg. Chem.* **1992**, *31*, 1600. (b) Hage, R.; Haasnoot, J. G.; Reedijk, J.; Wang, R.; Vos, J. G. *Inorg. Chem.* **1991**, *30*, 3263.

(9) (a) Danzer, G. D.; Golus, J. A.; Strommen, D. P.; Kincaid, J. R. *J. Raman Spectrosc.* **1990**, *21*, 3. (b) Vanderesse, R.; Lourak, M.; Fort, Y.; Caubere, D. *Tetrahedron Lett.* **1986**, *27*, 5483.

0002-7863/93/1515-8643$04.00/0

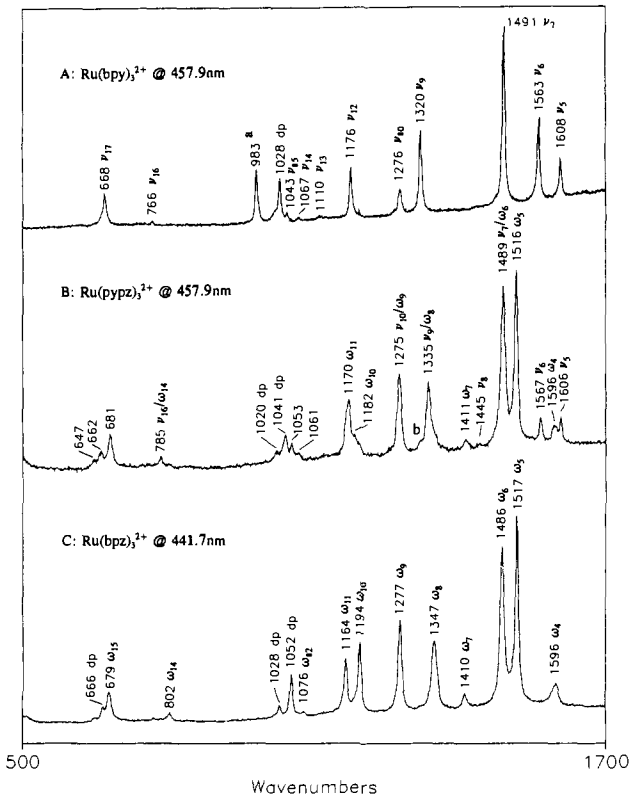

Figure 1. Resonance raman spectra: (a) band due to SO_4^{2-} which was used as an internal standard in this spectrum and (b) feature attributable to an impurity of bpy, due to the varying relative intensity of this feature from preparation to preparation; dp denotes polarized bands.

B. Preparation of the Complexes. The complexes Ru(bpy)$_3^{2+}$, Ru(bpy)$_2$(pypz)$^{2+}$, Ru(bpy-d_8)$_2$(pypz)$^{2+}$, and Ru(bpy-d_8)$_2$(3,5-d_2-pypz)$^{2+}$ were prepared as dichloride salts using previously reported procedures[5,11] and freshly sublimed ligands. The metal complexes were purified using established procedures.[11]

Spectral Measurements. RR and TR^3 spectra were acquired as described previously.[12] The RR spectra were obtained from solutions which were ~(1–4) × 10^{-3} M in metal complex. The 1004-cm^{-1} band of toluene (Aldrich) was scanned before the acquisition of the RR and TR^3 spectra to ensure correct positioning of the monochromator (±0.25 cm^{-1}). The monochromator was stepped using increments of 0.5 cm^{-1}.

The RR spectra were obtained using the excitation lines of a Spectra-Physics Model 2025-05 argon ion laser (457.9 nm), a Coherent Model Innova-100-K3 krypton ion laser (356.4 nm), or a Liconix Model 4240 helium cadium laser (441.7 nm). The TR^3 spectra were obtained with the third harmonic (354.7 nm) of a Quanta-Ray (Spectra Physics) Model DCR-3A Nd:YAG laser (operated at 20 Hz) or with the excitation lines resulting from Raman shifting either the second (532 nm) or the third harmonic of the Nd:YAG laser in a $^3/_4$-m Raman shifter containing 100 psi of hydrogen gas.

Results and Discussion

Ground-State Raman Spectra. The RR spectra of the tris-(homoleptic) complexes with the three pertinent ligands (bpy, bpz, and pypz) are given in Figure 1. The spectrum of Ru(bpy)$_3^{2+}$ has been thoroughly studied, and a reliable normal mode calculation, exploiting data for 12 isotopomeric analogues, has been reported.[12] The spectrum is appropriately interpreted in terms of a 21-atom unit (i.e., Ru(bpy)) possessing C_{2v} symmetry which gives rise to 20 Raman-active, totally symmetric modes. Four modes are associated with the C–H stretching coordinates and occur near 3000 cm^{-1}. There are seven (C–C) (and C–N) stretching coordinates which mix with four CCH (in-plane) bending coordinates to give rise to 11 modes between 1700 and 1000 cm^{-1}. These are labeled as ν_5–ν_{15} in trace A of Figure 1. Two other modes (ν_{16} and ν_{17}), which involve mainly CCC and CCN bending motions mixed with CCH bending and C–C and C–N stretching coordinates, are observed between 600 and 800 cm^{-1}.

The spectrum of the bipyrazine complex (trace C of Figure 1) can be interpreted similarly.[7] In this case, however, two of the CH units are replaced by N atoms and the 19-atom unit gives rise to 18 Raman-active, totally symmetric modes, the highest three being associated with the C–H stretching coordinates. The seven C–C and C–N coordinates mix with three (in-plane) CCH bending coordinates to give rise to 10 modes between 1700 and 1000 cm^{-1}. These are labeled as ω_4–ω_{13} in trace C of Figure 1 (we have designated the bipyrazine modes as ω_i in order to clarify the following discussion). As is the case with Ru(bpy)$_3^{2+}$, the bipyrazine complex exhibits two modes (ω_{14} and ω_{15}) between 600 and 800 cm^{-1}.

The spectrum of the homoleptic complex of 2-(2-pyridyl)-pyrazine is given in trace B of Figure 1. As is immediately apparent, the spectrum of this inherently asymmetric ligand can, to a great extent, be viewed as a composite of the spectra associated with the two symmetric ligands. Thus, one set of bands (labeled as ν_i) is associated with the pyridine fragment of the pypz ligand, while those labeled as ω_i appear at frequencies which are quite similar to those of coordinated bipyrazine and are thus ascribable to the pyrazine fragment. In the highest energy modes, the frequencies of each fragment are very close in energy to those observed for the symmetric ligands (traces A and C). Thus, ν_5, ν_6, and ν_8 and ω_4, ω_5, and ω_7 occur at frequencies which are within a few wavenumbers of their corresponding values in the complexes of the symmetric ligands. This "isolated vibrator" picture remains valid for most of the observed modes as can be seen by inspection of the spectra. However, there are several modes which apparently contain contributions from both fragments including that which occurs at 1335 cm^{-1}, which is most properly attributed to the so-called interring stretch (labeled as ν_9/ω_8). As expected, in the case of the pypz complex, this mode occurs at a frequency which is intermediate between the corresponding modes in the bipyridine and bipyrazine complexes. The other modes which appear at intermediate frequencies are those labeled as ν_7/ω_6 (1489 cm^{-1}), ν_{10}/ω_9 (1275 cm^{-1}), and ν_{16}/ω_{14} (785 cm^{-1}).

The only other modes in spectrum B which exhibit significant deviations from their values in traces A or C are the bands centered near 1170 cm^{-1}. The ω_{10} (1194 cm^{-1}) mode observed for Ru(bpz)$_3^{2+}$ (trace C) is observed at 1182 cm^{-1} in trace B, and the 1164-cm^{-1} (ω_{11}) mode (trace C) shifts to 1170 cm^{-1} for Ru(pypz)$_3^{2+}$. The "bpy" mode expected to occur near 1176 cm^{-1} (ν_{12}) is apparently observed, by near coincidence, with the 1170-cm^{-1} feature. The modes below this frequency region (especially in the TR^3 spectra, vide infra) are often too weak to be observed and assigned. While this was possible in the case of Ru(bpy)$_3^{2+}$, with the aid of an extensive data set involving 12 isotopomers, sufficient data are not available in the present cast to accomplish this. In any case, complete data are not required to establish the essential points of this work. Thus, modes which occur below ~1200 cm^{-1} are not discussed in detail here. The only exception to this is the relatively clear identification of the isolated bands occuring at 802 cm^{-1} (ω_{14}) in the spectrum of Ru(bpz)$_3^{2+}$ and at 766 cm^{-1} (ν_{16}) in the spectrum of Ru(bpy)$_3^{2+}$ which is observed at 785 cm^{-1} (ν_{16}/ω_{14}) in the spectrum of Ru(pypz)$_3^{2+}$. This is useful information inasmuch as the corresponding "radical" mode is relatively strong and easy to identify in the TR^3 spectra (vide infra).

(10) McClanahan, S.; Kincaid, J. *J. Raman Spectrosc.* **1984**, *15*, 173.
(11) (a) Braddock, J. N.; Meyer, T. J. *J. Am. Chem. Soc.* **1973**, *95*, 3158. (b) Sprintschnick, G.; Sprintschink, H. W.; Kirsch, P. P.; Whittwn, D. G. *J. Am. Chem. Soc.* **1977**, *99*, 4947. (c) Crutchley, R. J.; Lever, A. B. P.; Poggi, A. *Inorg. Chem.* **1983**, *22*, 2647.
(12) Strommen, D. P.; Mallick, P. K.; Danzer, G. D.; Lumpkin, R. S.; Kincaid, J. R. *J. Phys. Chem.* **1990**, *94*, 1357.

Table I. Ground- and ^{3}MLCT-State Frequencies

mode	$Ru(bpy)_3^{2+}$, $Ru(bpz)_3^{2+}$ (Δd)[a]	$[Ru(bpz)_3^{2+}]^*$, $[Ru(bpz)_3^{2+}]^*$ (Δd)[a]	$\Delta\nu$,[c] $\Delta\omega$[d]	$Ru(pypz)_3^{2+}$ (Δd)[b]	$[Ru(pypz)_3^{2+}]^*$ (Δd)[b]	$\Delta\nu$,[c] $\Delta\omega$,[d] $\Delta\nu/\omega$[e]
ν_5/ν_5'	1608 (23)	1548 (21)	−60	1606 (19)	1590 (16)	−18
ω_4/ω_4'	1596	1538	−58	1596 (0)	1537 (2)	−57
ν_6/ν_6'	1563 (19)	1506 (16)	−57	1567 (15)	1522 (13)[h]	−45
ω_5/ω_5'	1517	1496	−21	1516 (4)	n.o.[h,i]	−20
ν_7/ν_7'	1491 (27)	1495 (21)	4			
$\nu_7/\omega_6/\nu_7'/\omega_6'$				1489 (14)	1464 (27)	−29
ω_6/ω_6'	1486	1430	−56			
ν_8/ν_8'	1450 (68)[g]	1427 (32)	−23	1445 (60)	1435 (26)	−10
ω_7/ω_7'	1410	1409	−1	1411 (3)	1409 (13)	−2
ν_9/ν_9'	1320 (24)	1365 (44)	45	(1290)		
$\nu_9/\omega_8/\nu_9'/\omega_8'$				1335	1355 (25)	20
ω_8/ω_8'	1347	1359	12	(1328)		
ν_{10}/ν_{10}'	1276 (20)	1285 (17)	9	(1254)		
$\nu_{10}/\omega_9/\nu_{10}'/\omega_9'$				1275	1276 (13)	1
ω_9/ω_9'	1277	1272	−5	(1278)		
ν_{11}/ν_{11}'	1264 (52)[g]	1212 (58)	−52	1265 (30)[g]	1254 (19)	−21
ω_{10}/ω_{10}'	1194	1223	29	1182	1213 (10)	31
ν_{12}/ν_{12}'	1176 (93)	1164 (97)	−12	n.o.	1162 (74)	−20
ω_{11}/ω_{11}'	1164	1148	−16	1170 (0)	1149 (0)	−21
ν_{13}/ν_{13}'	1110 (94)	1100 (110)	−10			
ω_{12}/ω_{12}'	1076	1063	−13			
ν_{14}/ν_{14}'	1067 (158)	1028 (130)	−39			
ω_{13}/ω_{13}'	1067[g]	1043	−24			
ν_{15}/ν_{15}'	1043 (176)	1014 (163)	−29			
ω_{14}/ω_{14}'	802	772	−30			
$\nu_{16}/\omega_{14}/\nu_{16}'/\omega_{14}'$				785	765 (1)	−20
ν_{16}/ν_{16}'	766 (8)	742 (8)	−24			
ω_{15}/ω_{15}'	679	675	−4			

[a] Observed deuterium shift for $Ru([3,3',5,5'-^2H_4]bpy)_3^{2+}$. [b] Observed deuterium shift for *3,5-d_2*-pypz in the complex $Ru(bpy)_2(3,5\text{-}d_2\text{-pypz})^{2+}$. [c] $\Delta\nu = \nu_i' - \nu_i$. [d] $\Delta\omega = \omega_i' - \omega_i$. [e] $\Delta\nu/\Delta\omega = \nu_i'/\omega_i' - \nu_i/\omega_i$. [f] Observed frequency for *3,5-d_2*-pypz in the complex $Ru(bpy)_2(3,5\text{-}d_2\text{-pypz})^{2+}$. [g] Observed with near π–π^* excitation (e.g, 356.4 nm). [h] Alternatively assignable to ω_5' or mixing of ν_6'/ω_5'. [i] n.o. denotes not observed.

In summary of this section, while most of the features observed in the spectrum of the pypz complex can be interpreted as being associated with vibrations isolated on the separate fragments, a few are best described as modes which involve motions of both fragments. It is satisfying to note that the features which appear at intermediate frequencies are precisely those that are assigned to motions of the "central-bonds" atoms in the previously reported normal mode calculations.[12] Thus, in the case of $Ru(bpy)_3^{2+}$, ν_7(1491), ν_9(1320), ν_{10}(1276), and ν_{16} (766) were seen to involve mainly the C_2–$C_{2'}$, C_2–C_3, and C_2–N stretching and C_2C_3H bending coordinates. While a separate normal mode calculation of the asymmetric pyridylpyrazine complex would be necessary to precisely define the coordinate contributions to these modes in the pypz complex, to the extent that the C_2–C_3 and C_2–N bonds of this ligand are similar to those of the bipyridine and bipyrazine ligands, the mode compositions are expected to be similar.

In order to provide support for this interpretation of the ground-state spectrum of the pypz complex and to clarify assignments of the ^{3}MLCT-state spectrum (vide infra), we have acquired the spectra of the deuteriated analogue [3,5-$^2H_2$]-2-(2-pyridyl)-pyrazine (*3,5-d_2*-pypz). The frequency shifts observed upon deuteriation are given in Table I along with the observed frequencies for all of the complexes of interest. As can be seen by inspection of the observed deuterium shifts, most of the modes ascribable to the pyrazine fragment exhibit only very small, or negligible, shifts. The "pyridine" modes on the other hand exhibit shifts which are comparable to those previously documented for complexes of [3,3',5,5'-$^2H_4$]bipyridine (these latter shifts are also given in the table for comparison purposes). The only modes of the pyridylpyrazine complex which deviate from this behavior are the ones referred to above, i.e., ν_7/ω_6, ν_9/ω_8, ν_{10}/ω_9, and ν_{16}/ω_{14}. These modes involve contributions from the central atoms of both fragments in the natural abundance species but in some cases (ν_9/ω_8 and ν_{10}/ω_9) may split to yield two separate bands upon deuteriation of the 3- and 5-positions of the pyridine ring.

Excited-State Spectra. A. Differentiation of "Radical" and "Neutral Ligand" Modes. The TR^3 spectra of the tris(pyridylpyrazine) complex are given in Figure 2 along with the near-UV excited ground-state RR spectrum (trace A). Time-resolved RR spectra were obtained at several excitation wavelengths in order to distinguish between modes (labeled, pypz) which are associated with the coordinated "radical" and those which are ascribable to the remaining two "neutral ligands". This is possible because the radical-like ligand which carries the optical electron density is expected to possess a π–π^* transition in the region between 360 and 380 nm, while the remaining two coordinated neutral ligands exhibit π–π^* transitions near 320 nm.[13]

As can be seen by inspection of Figure 2, the TR^3 spectra are entirely consistent with these expectations. Thus, the spectrum acquired with excitation near 320 nm (trace B) exhibits features which are clearly ascribable to the coordinated neutral ligands, their frequencies and intensities being quite similar to those in the spectrum of the ground state (trace A). On the other hand, in the TR^3 spectrum acquired with excitation near 370 nm (in resonance with the radical π–π^* transition expected in this region), a different set of features now dominates. These new features are characteristic of a radical-like coordinated ligand. A careful analysis of the details of these latter features is necessary to reveal the precise nature of this radical-like ligand (vide infra). Finally, the TR^3 spectrum acquired with excitation at 354.7 nm demonstrates that both sets of features are enhanced at this intermediate excitation energy.

B. Analysis of "Radical" Features. The TR^3 spectrum of the pypz complex acquired with 354.7-nm excitation (wherein the features of all three coordinated ligands are enhanced) is obviously quite complex. In order to provide definitive assignments of all the observed features, it is necessary to compare the spectrum with those of strategically chosen "reference" complexes and several deuteriated analogues. These spectra are given in Figures 3 and 4, and the observed frequencies for the radical fragments

(13) Braterman, P. S.; Harriman, A.; Health, G. A.; Yellowlees, L. *J. Chem. Soc., Dalton Trans.* **1983**, 1801.

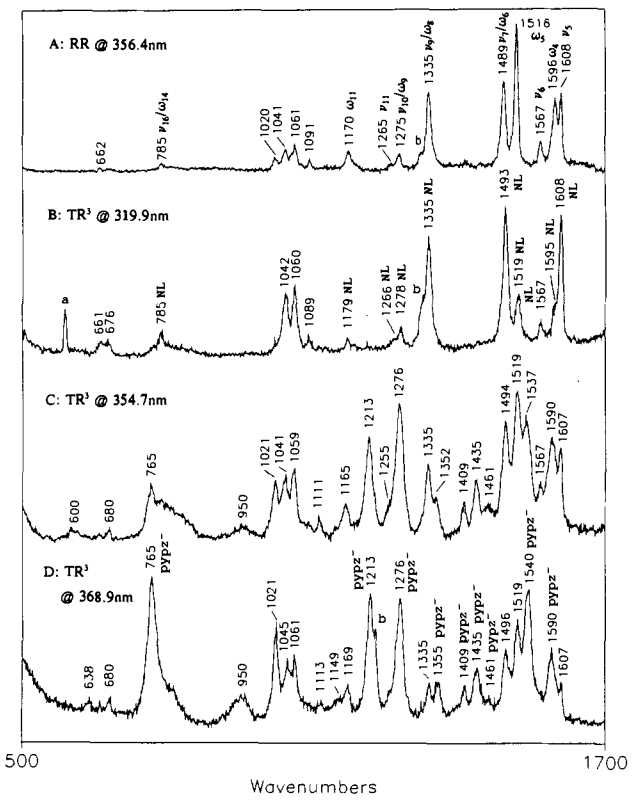

Figure 2. RR and TR^3 spectra of $Ru(pypz)_3^{2+}$: (a) band resulting from a rotational line of H_2 from Raman shifting and (b) feature attributable to an impurity of bpy (traces A and B) or bpz (trace D), due to the varying relative intensity of this feature from preparation to preparation.

are given in Table I along with those of other pertinent reference complexes (e.g., $Ru(bpy)_3^{2+}$, $Ru([3,3',5,5'\text{-}^2H_4]bpy)_3^{2+}$, and $Ru(bpz)_3^{2+}$).

The TR^3 spectrum of the tris(pyridylpyrazine) complex is given in trace B of Figure 3 along with those of $Ru(bpy)_3^{2+}$ (trace A) and $Ru(bpz)_3^{2+}$ (trace C). The most striking observation upon comparison of the three spectra is the increased spectral complexity in the case of the inherently asymmetric complex $Ru(pypz)_3^{2+}$. Also, there are no features which can be clearly attributed to "bipyridine-radical" modes. Instead, the set of features identified as being associated with the radical ligand (i.e., those which maximize at 368.9 nm in Figure 2) appears itself to be comprised of three subsets of modes. One subset, labeled as ω_i' in trace B of Figure 3, appears to be similar in frequency and intensity to that of the bipyrazine radical (labeled ω_i' in trace C). A second subset, labeled as ν_i'/ω_i' in trace B, is ascribable to the central-atom vibrations. The other subset of bands (labeled as x_i in trace B of Figure 3) is not clearly identifiable as either bpy-like modes or "neutral bpy" modes. Of these latter bands, the most clearly evident are those that occur at 1590, 1519, 1435, and ~1254 cm^{-1}.

In order to properly assign these new features (labeled as x_i in trace B) to a particular fragment of the coordinated pypz radical, a number of reference compounds, whose spectra are given in Figure 4, were studied. The spectrum given in trace A is that of the tris(pyridylpyrazine) complex. As was pointed out above, it consists of a set of features associated with the two neutral pypz ligands (labeled as NL in trace A) and a set of radical-like features. These latter bands are ascribable to coordinated pypz and are the essential data which provide structure information for the localized excited state.

The spectrum shown in trace B is that of the heteroleptic complex $Ru(bpy)_2(pypz)^{2+}$. In this complex, it is expected that the ^{3}MLCT-state electron density is localized on the coordinated pypz, on the basis of previously reported studies of heteroleptic complexes of ruthenium with bipyridine and bipyrazine.[7] The TR^3 spectrum of this complex (trace B) is indeed consistent with the formulation $Ru^{3+}(bpy)_2(pypz)$. Thus, no modes which are considered to be characteristic of coordinated bpy are observed (i.e., those labeled as ν_i' in Figure 3, trace A). It is also apparent from inspection of trace B that the modes labeled as x_i persist in this derivative, demonstrating that they are associated with the coordinated pypz ligand as was implied in the excitation profile study shown in Figure 2.

Inasmuch as the subset of pypz modes which are labeled as ω_i' in Figure 3 (trace B) is quite similar in frequency and intensity to the bpz radical modes (labeled as ω_i' in trace C of Figure 3), it is most reasonable to attribute the new features (labeled as x_i) to modes associated with the pyridine fragment of the coordinated pypz which are apparently shifted from their values in a coordinated neutral (or radical) bipyridine. It should be pointed out that any pyridine modes associated with the $pypz^-$ ligand which exhibit frequencies similar to those normally observed for bpy-like modes would be hidden by overlap with the neutral ligand modes of the remaining two coordinated neutral bpy ligands in the complexes whose spectra are given in traces A and B of Figure 4. In order to reveal such features, the TR^3 spectrum of the corresponding heteroleptic complex with $[^2H_8]$bipyridine (bpy-d_8) was obtained and is given in trace C of Figure 4. In this case, the neutral ligand modes (i.e., those associated with the bpy-d_8 ligands) occur at well-known values which are not coincident with those of natural abundance bpy-like modes.[10,12] Again, it is clear that the ^{3}MLCT state of this complex is properly formulated as $[Ru^{3+}(bpy\text{-}d_8)_2(pypz^-)]^{2+}$, i.e., there is no evidence for formation of the $[Ru^{3+}(bpy\text{-}d_8)(bpy\text{-}d_8^-)(pypz)]^{2+}$ formulation inasmuch as no bands characteristic of a radical-like bpy-d_8 ligand are observed.[12] Furthermore, it is important to note that the 1608-cm^{-1} bpy-like mode is absent while the 1590-cm^{-1} feature persists (vide infra).

The last spectrum given in Figure 4 (trace D) is that of the deuteriated pyridylpyrazine complex which can be directly compared with the spectrum of its nondeuteriated analogue (trace B). In this case, it is expected that any features which are associated with the pyridine fragment of the pypz ligand will experience a shift upon deuteriation.

It is most useful to carefully compare the three spectra given in traces B, C, and D. In trace B, many features which are characteristic of coordinated (natural abundance) bipyridine are observed and appropriately labeled as NL. The strong features observed at 1590 and 1522 cm^{-1} as well as the weaker features evident at 1461 and 1254 cm^{-1} are clearly not associated with the coordinated bipyridines inasmuch as they persist in the spectrum of $Ru(bpy\text{-}d_8)_2(pypz)^{2+}$ (trace C). Thus, they are associated with the $pypz^-$ ligand. In addition, the elimination of the strong 1607-cm^{-1} feature in trace C (ν_5 occurs at 1572 cm^{-1} in trace C) does confirm the absence of any feature at approximately 1608 cm^{-1}.

The above comparison of traces B and C indicates that, in addition to the set of bpz radical-like bands (ω_i'), the $pypz^-$ ligand exhibits the set of features labeled x_i which are most likely associated with the pyridine fragment of $pypz^-$. Careful comparison of traces C and D supports this interpretation. It is for this reason that the new features are labeled as ν_i'' in trace D. The essential rationale behind utilizing *3,5-d_2*-pypz is that deuteriation of the pyridine fragment is expected to induce shifts in the ν_i'' modes which should be comparable to those previously reported for $[3,3',5,5'\text{-}^2H_4]$bpy.[12] To the extent that the modes of the pyridine fragment of $pypz^-$ are similar to those of a coordinated bpy, similar deuterium shifts are expected, although some differences can result inasmuch as the frequencies (and the precise mode formulations) may be slightly different.

In general, the observed deuterium shifts provide convincing support. Thus, the 1590-cm^{-1} feature (x_1) seen in trace C shifts

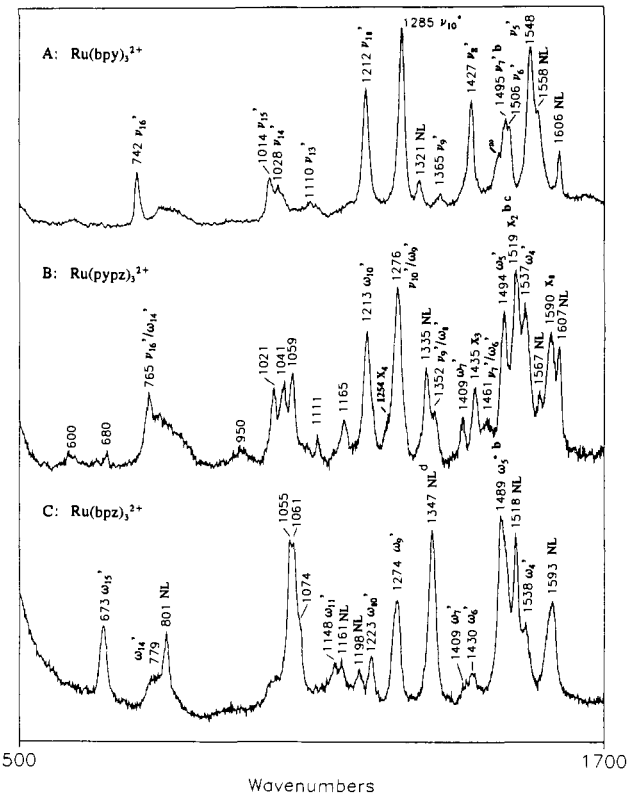

Figure 3. TR^3 spectra of Ru(bpy)$_3^{2+}$, Ru(pypz)$_3^{2+}$, and Ru(pypz)$_3^{2+}$ acquired with 354.7-nm excitation: (a) feature assigned as $2 \times \nu_{16}'$ (1482 cm^{-1}) (ref 12); (b) also contains contributions from a neutral ligand (NL) mode; (c) mode assigned as x_2 based on the appearance of this feature in the TR^3 spectrum of the Ru(bpy)$_2$(pypz)$^{2+}$ complex (trace B, Figure 4); and (d) also contains contribution from ω_8'.

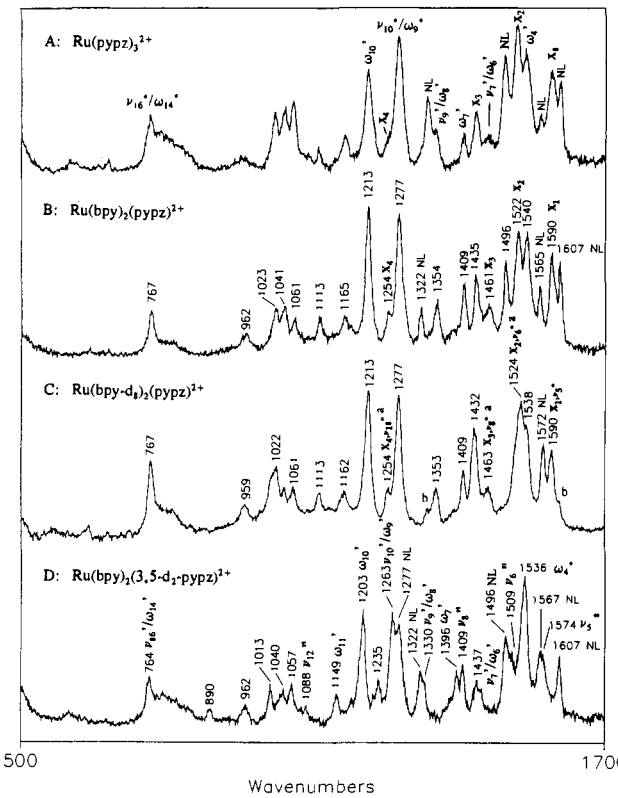

Figure 4. TR^3 spectra of Ru(pypz)$_3^{2+}$ and strategically chosen reference complexes acquired with 354.7-nm excitation: (a) may also contain contribution from a bpy-d_8 neutral ligand (NL) mode and (b) features that vary in relative intensity from preparation to preparation and are ascribable to a slight impurity of Ru(bpy-d_8)$_2$(bpy)$^{2+}$.

to ~1574 cm^{-1} (where it is now labeled as ν_5''), a shift of 16 cm^{-1} in reasonable agreement with the corresponding shift of ν_5' in the case of the [3,3',5,5'-$^2H_4$]bipyridine complex (Table I). The next two modes associated with the pyridine fragment of pypz occur at 1522 and 1435 cm^{-1} and are labeled as x_2 and x_3 in traces A–C and ν_6'' and ν_8'' in traces C and D. The derived deuterium shifts of these two modes are also in satisfactory agreement with the corresponding shifts observed for the Ru(bpy)$_3^{2+}$/Ru([3,3',5,5'-$^2H_2$]bpy)$_3^{2+}$ pair (Table I). Similar agreement is noted for the 1254-cm^{-1} feature (ν_{11}'') observed in traces B and C which shifts to 1235 cm^{-1} in trace D.

Several pypz$^-$ modes warrant special attention. The modes observed at 1461, 1355, 1276, and 785 cm^{-1} are radical-like modes which contain significant contributions from the central-atoms region of the molecule, according to a previously reported normal mode calculation[12] for Ru(bpy)$_3^{2+}$ (this interpretation is valid to the extent that the central bonds of pypz are similar to those of bpy). These central-bonds vibrations are expected to downshift upon deuteriation owing to contributions from the $C_2C_3^2H$ bending coordinate. In fact, these pypz modes do exhibit significant shifts upon deuteriation of the pyridine fragment. Thus, ν_9'/ω_8' shifts from 1355 (traces B and C) to 1330 cm^{-1} (trace D), while ν_7'/ω_6', ν_{10}'/ω_9', and ν_{16}'/ω_{14}' also exhibit downshifts.

C. Structural Interpretation of the TR^3 Spectrum. The above analysis argues that in the ^{3}MLCT state of these complexes, the optical electron density is polarized toward the pyrazine fragment, giving rise to a set of pypz modes which are quite similar in frequency and intensity to the corresponding modes of a coordinated bpz ligand as well as to a set of features which are attributable to the pyridine fragment of the coordinated pypz ligand. These latter features occur at frequencies which are different from their corresponding values for either a coordinated bpy or a coordinated bpy. Two of the modes associated with the periphery of the pyridine fragment (ν_5 and ν_6) shift down upon formation of the pypz$^-$ as they do in the case of bpy formation but only by a fraction of the shift observed in the case of bpy formation (i.e., 18 vs 60 cm^{-1} and 45 vs 57 cm^{-1}). The modes associated with the central-atoms region of the pypz ligand (i.e., ν_7/ω_6, ν_9/ω_8, ν_{10}/ω_9, and ν_{16}/ω_{14}) all exhibit shifts upon formation of pypz$^-$ which are approximately intermediate between the shifts observed for the Ru(bpy)$_3^{2+}$/[Ru(bpy)$_3^{2+}$]* and Ru(bpz)$_3^{2+}$/[Ru(bpz)$_3^{2+}$]* pairs. Thus, the observed $\nu_7 \rightarrow \nu_7'$ shift is 4, and the observed $\omega_6 \rightarrow \omega_6'$ shift is –56 cm^{-1}, while the observed $\nu_7/\omega_6 \rightarrow \nu_7'/\omega_6'$ shift is –29 cm^{-1}. Similarly, the $\nu_9/\omega_8 \rightarrow \nu_9'/\omega_8'$ shift is 20 cm^{-1}, while the corresponding $\nu_9 \rightarrow \nu_9'$ and $\omega_8 \rightarrow \omega_8'$ shifts are 45 and 12 cm^{-1}, respectively. In the case of $\nu_{10}/\omega_9 \rightarrow \nu_{10}'/\omega_9'$, the shift is 1 cm^{-1} compared to 9 and –5 cm^{-1}, for the $\nu_{10} \rightarrow \nu_{10}'$ and $\omega_7 \rightarrow \omega_7'$ shifts, respectively.

In summary of this section, on the basis of the above analysis, the picture of a pypz-localized ^{3}MLCT state that emerges is that of a asymmetric charge distribution in which electron density is polarized toward the pyrazine fragment of the coordinated pypz. In agreement with previous TR^3 studies of symmetrical chelates, population of the (net anti-bonding) LUMO of the chelate results in a general lowering of the vibrational modes, as expected, but the polarized charge distribution substantially alters the observed frequency shifts compared to that in the symmetrical chelates. In the present case (pypz$^-$), this polarization effect is most clearly manifested in the relatively small downshifts observed for the ν_6/ν_6' and, especially, ν_5/ν_5' modes.

Photochemical and Photophysical Implications. During the past decade, RR and TR^3 methods have played an increasingly important role in defining the structural basis of the inherent photophysical properties of this class of complexes. The earliest TR^3 studies[2,3] provided convincing evidence for a single chelate-localized ^{3}MLCT state in the case of Ru(bpy)$_3^{2+}$, a symmetric tris(homoleptic) complex. Subsequent studies of heteroleptic

analogues consisting of two distinct types of bipyridine-related ligands documented selective populations of ^{3}MLCT states centered on the most easily reduced member of the mixed ligand pair.[5-7]

The present work represents the first attempt to precisely define the structural details of ^{3}MLCT states involving ligands which are inherently asymmetric. The essential contribution of this study is to convincingly demonstrate the impressive capability of RR and TR^3 methods to interrogate these states and to document, for the first time, polarization of ^{3}MLCT-state electron density, an effect which results in further localization of charge. In fact, RR and TR^3 methods seem uniquely suited to reveal these subtle structural/electronic features which play a role in dictating photophysical properties.

This issue of ^{3}MLCT-state polarization carries important implications for many of the photophysical and photochemical properties of these systems. Thus, studies have recently begun to appear which are focused on the use of such inherently asymmetric complexes to fine-tune photophysical properties as an attempt to eliminate undesirable photochemistry,[8a] and a further definition of ^{3}MLCT-state structural details, as provided here, is of obvious relevance. In addition, there is an increasing number of studies which incorporate these types of complexes into synthetic supramolecular systems via attachment through peripheral functionalities.[16] To the extent that such functionalization may inadvertently induce ^{3}MLCT-state polarization, the interpretation of photophysical properties may be compromised unless this effect is explicitly considered.

Finally, while the present study deals with complexes of ligands which are inherently asymmetric, the possibility exists that asymmetry may be environmentally induced. This is an important consideration for the large number of studies which incorporate members of this class of complexes into various types of organized assemblies,[17] including zeolites[18] and glasses,[19] where asymmetry may be environmentally induced by site asymmetry of the host material. In any case, it seems clear from the present work that RR and TR^3 methods are entirely capable of revealing such polarization effects.

Acknowledgment. This work was supported by a grant from the Department of Energy, Office of Basic Energy Sciences (Grant ER13619). Such support does not constitute an endorsement by DOE of the views expressed in this work.

(14) Allen, G. H.; White, R. P.; Rillema, D. P.; Meyer, T. J. *J. Am. Chem. Soc.* **1984**, *106*, 26B.

(15) (a) Mallick, P. K.; Strommen, D. P.; Kincaid, J. R. *J. Am. Chem. Soc.* **1990**, *112*, 1686. (b) Chisholm, M. H.; Huffman, J. C.; Rothwell, I. P.; Bradley, P. G.; Kress, N.; Woodruff, W. H. *J. Am. Chem. Soc.* **1981**, *103*, 4945.

(16) (a) Yonemoto, E. H.; Riley, R. L.; Kim, Y. I.; Atherton, S. J.; Schmehl, r. H.; Mallouk, T. E. *J. Am. Chem. Soc.* **1992**, *114*, 8081. (b) Larson, S. L.; Cooley, L. F.; Elliott, C. M.; Kelley, D. F. *J. Am. Chem. Soc.* **1992**, *114*, 9504. (c) Ryu, C. K.; Wang, R.; Schmehl, R. H.; Ferrere, S.; Ludwikow, M.; Merkert, J. W.; Headford, C. E. L.; Elliott, C. M. *J. Am. Chem. Soc.* **1992**, *114*, 430. (d) Ohno, T.; Nozaki, K.; Haga, M. *Inorg. Chem.* **1992**, *31*, 4256.

(17) Mallouk, T. E.; Lee, H. *J. Chem. Ed.* **1990**, *67*, 829.

(18) (a) Turbeville, W.; Robins, D. S.; Dutta, P. K. *J. Phys. Chem.* **1992**, *96*, 5024. (b) Dutta, P. K.; Turbeville, W. *J. Phys. Chem.* **1992**, *96*, 9410. (c) Incavo, J. A.; Dutta, P. K. *J. Phys. Chem.* **1990**, *94*, 3075. (d) Dutta, P. K.; Incavo, J. A. *J. Phys. Chem.* **1987**, *91*, 4443. (e) Maruszewski, K.; Strommen, D. P.; Handrich, K.; Kincaid, J. R. *Inorg. Chem.* **1991**, *30*, 4579. (f) Maruszewski, K.; Strommen, D. P.; Kincaid, J. R. *J. Am. Chem. Soc.*, in press.

(19) Shi, W.; Wolfgang, S.; Strekas, T. C.; Gafney, H. D. *J. Phys. Chem.* **1985**, *89*, 974.